Armenian Journal of Physics, 2013, vol. 6, issue 4, pp. 177-187

$Ba_xSr_{1-x}TiO_3$/pc-Si HETEROJUNCTION

V. BUNIATYAN[1], C. HUCK[2], A. POGHOSSIAN[2], V.M. AROUTIOUNIAN[3], and M.J. SCHOENING[2]

[1]State Engineering University of Armenia (SEUA), Yerevan
[2] FH Aachen, Campus Julich, Institute of Naño - and Biotechnologies, Julich, Germany
[3] Yerevan State University (YSU)
E-mail: vbuniat@seua.am

Received 10 November 2013

An amorphous $Ba_xSr_{1-x}TiO_3$/pc - Si (polycrystalline silicon) anisotropic heterojunction was systematically investigated in terms of built-in potentials, interface potentials and space - charge depletion layer widths. The presence of oxygen vacancies as well as the non-linear dependence of the dielectric permittivity of ferroelectric films on the electric field is considered for different values of oxygen vacancies and doping levels in silicon.

1. Introduction

In last decade, increasing attention was attributed to heterojunctions based on ferroelectric and multiferroic films grown on semiconductors. Such heterojunctions belong to a novel class of solid-state devices and are expected to be promising candidates with large potential for new multifunctional device applications [1-5]. Most of our studies which concern amorphous ferro/crystalline and crystalline - ferro/crystalline - semiconductor heterojunctions have mainly experimental character and the aim to detect and verify atomic structure, band offsets, current - flow mechanisms as well as photovoltaic and polarization properties. There are few reports where the electro-physical and optical properties of ferro/semiconductor heterojunctions are systematically and accurately studied in a theoretical manner.

In these studies the influence of structural defects like oxygen vacancies, the non-linear dependence of the dielectric permittivity of ferroelectric thin films on the electric field as well as Pool-Frenkel ionization (at high electric fields) processes on various properties and characteristics of ferro-/semiconductor heterojunctions are not taken into account. Currently, it is well established that oxygen vacancies play a major role [6-12]. The oxygen concentration is not constant throughout the film. Near the metal electrodes and phase transition layer the oxygen concentration decreases sharply [6-8] approximately to 50% of its original value in the center (~20 nm from the metallic electrode surface). In oxide - perovskite ferroelectrics there are three oxygen ions per unit cell. The density of the oxygen ions in the bulk of the film amounts to $1.5\cdot10^{28}$ m^{-3}, while in a 20 nm thick 50% depleted (by oxygen) interface layer it is about $3\cdot10^{20}$ m^{-3}. The lack of oxygen results in the image charge on the metal electrode or the phase-transition interface layer. As a consequence, the increased density of oxygen vacancies at the interface leads to a dipole-layer lowering the electric field in the film. The non-uniform distribution of oxygen vacancies near the interfaces causes bending of the energy bands and changes the shape of the barrier. At high temperatures, the oxygen vacancies are double ionized,

each supplying two electrons to the conduction band. Oxygen vacancies act as donors [7, 8] causing n-type conductivity. In the neutral state, the donor level is double occupied and there is reduced repulsive interaction between the vacancy and neighboring cations. The interfacial vacancies cause distortion of the crystal lattice and polarization fields around the vacancy. This makes the levels deeper and causes them to act as charge traps. The concentration of charge trapped can change from 10^{16} cm^{-3} to $4 \cdot 10^{17}$ cm^{-3} and higher (up to ~10^{22} cm^{-3}) [6-10]. However, not all oxygen vacancies trap electrons. The interfacial built-in electric field associated with the trapping centers and oxygen vacancies results in changes in the interfacial permittivity of the films [11, 12]. The oxygen vacancies are not the main and only defect of ferroelectric films. The Ba, Sr vacancies in BST result in shallow acceptor levels [6, 11]. Dopants also result in levels in the forbidden band. Nb gives a shallow level, while Mn, Mg, Cr, Pt and Fe exhibit levels near the midgap [7, 8]. Thus, for a low density of oxygen vacancies the non-doped ferroelectric titanate films are considered to have slightly p-type conductivity due to background impurities (i.e. Na^{+} for Pb^{+2}, Fe^{+3} for Ti^{+4}) and the regions rich in oxygen vacancies (interfaces) have n-type conductivity.

In this paper we present systematic calculations of built-in potentials, its distribution across the junction and depletion widths of $Ba_xSr_{1-x}TiO_3$/pc-Si heterojunction where the following is taken into account:

a) the dielectric permittivity of ferroelectric films is non-linear dependent on the electric field $\mathcal{F}$;

$$\varepsilon(\mathcal{F}, r) = \varepsilon(0)(1 + A\mathcal{F}^2\,(x))^{-1},$$

where $A = 3\beta$ $[\varepsilon_0\varepsilon]$, ε_0 is the vacuum dielectric constant, ε (0) is the permittivity at zero bias. For example, for $SrTiO_3$, $\beta = 8 \cdot 10^9$ Vm^5/C, ε (0) = 300 and $A = 0.45 \cdot 10^{-15}$ $(m/V)^2$[11];

b) some point defects in ferroelectric materials such as inevitable presented oxygen vacancies create energy levels for charge carriers in the band gap of ferroelectrics. In particular, deep-level trapping states with energies in the range of E_v = 2.4 eV to E_v = 3.15 eV lie near the valence band and a series of shallow traps linear the conduction band edge in the range of $E_C - E_{tn}$ = 0.06 - 0.4 eV. These electron traps are attributed to oxygen vacancy or iron transition metal/ oxygen vacancy defects [6-12];

c) the high concentration of oxygen vacancy “endows” ferroelectric n-type semiconductor properties and due to the low concentration/non-vacancy ferroelectric core exhibit p-type properties [6-12];

d) the traps release electrons under an applied DC field via the Pool-Frenkel mechanism and become charged. As a consequence, the trapped electron occupation (distribution f(Φ)) function is changed due to the charge of oxygen vacancies “conditioned” electron levels and new high electric field polarized includes are formed in films. The electric field of a point charge polarizes the crystal locally reducing its permittivity [6, 7, 12].

2. Theoretical modeling

For theoretical modeling, the metal contacts of the M-BST/c-pSi-M structure are considered as nearly Ohmic (or Schottky) contacts. The "core" far away from the ferroelectric heterojunction interface exhibits p-type conductivity and the heterojunction surface in contact to crystalline pc-Si exhibits n-type conductivity due to a high oxygen vacancies concentration. Furthermore, it is assumed that, in the band gap of ferroelectric near the conduction band, there are donor-like electron-trap levels conditioned mainly by oxygen vacancies (other possible defects, such as strain, interstitial atomic (structural) defects are not considered in this paper) and near the top of valence band there exist hole-trap levels, conditioned by other acceptor like defects. Both of the trap levels are exponentially distributed in the band gap of ferroelectric films. Below the activation temperature ($T<T_a$) and without an external electric field, the oxygen vacancies are neutral (occupied by electrons) and cause elastic deformation of the lattice. In the energy diagram shown in Figure 1, it is assumed that trap levels have concentrations N_{tn} (for electrons) and N_{tp} (for holes) with the characteristic energies E_{tn} and E_{tp} below the conductive and up to valence band edges of BST, respectively. Based on the results obtained in [6, 8, 9], we have adopted the values of $E_{c1}–E_{tn} \approx 0.06$-0.4 eV, $N_{tn} \approx 10^{16}\div10^{19}$ cm^{-3} and $E_{tp} \approx E_{v1}$ +1.2 eV, $N_{tp\approx}(10^{13}\div 10^{14})$ cm^{-3}, for this consideration (Fig. 1). It is well known [13-15] that the transition between the two materials at the heterojunction interface causes energy discontinuities in the conduction and valence bands, ΔE_c and ΔE_v, in the vicinity of the metallurgical junction. In addition, a dipole layer may appear at the junction and various kinds of imperfections at the interface may result in an interface change.

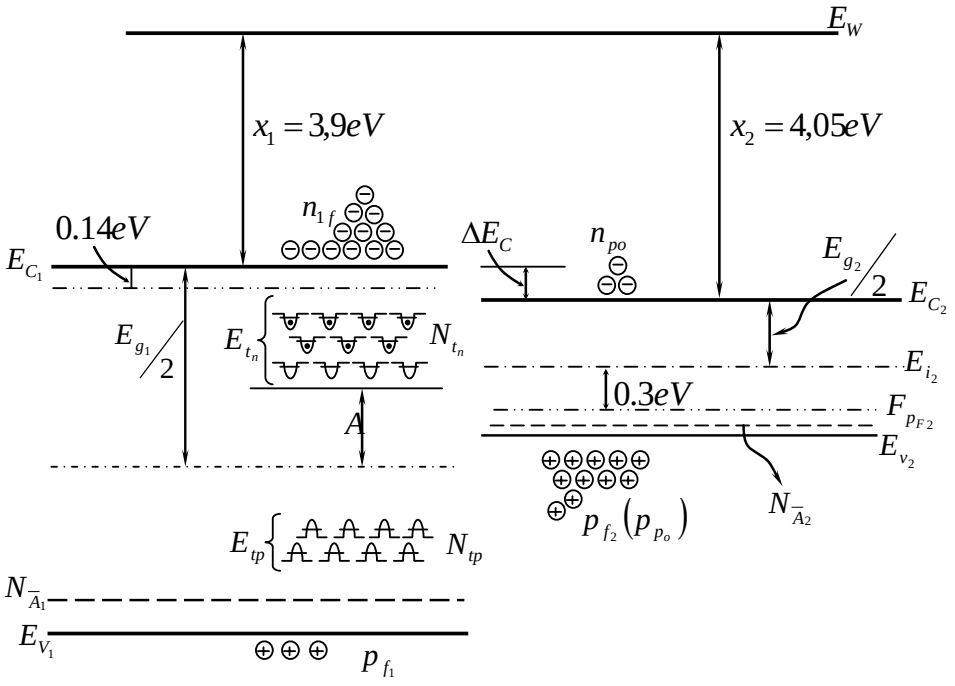

Fig.1. Relative band alignments with respect to the vacuum level for BST and pc-Si before heterojunction formation (if $N_{A2}^{-}\approx 2\cdot10^{15}$cm^{-3} , $F_{pF2}\approx$0.31 eV below E_{i2}, $n_{f1}\approx 10^{17}$ cm^{-3}, $F_{nF1}\approx$0.14 eV below E_{c1},$E_{c1} = E_{g1}/2 = 1.6$ eV).

Our theoretical calculations have been done for $Ba_{0.25}Sr_{0.75}TiO_3$/cp-Si heterojunction where Si <100> with $\rho \approx 5$ - 10 Ωcm is doped with boron B, the band gap of BST and Si are 3.2 eV and 1.1 eV, respectively, the electron affinities are about 3.9 eV and 4.05 eV, respectively. p - Si with a resistivity of $\rho \approx 7$ Ωcm corresponds to an acceptor concentration of $N_{A2}^- \approx 2 \cdot 10^{15}$ cm^{-3} and Fermi-quasilevel located at 0.31 eV below from the midgap (intrinsic Fermi level E_{i2}) and the work function of p-Si becomes 4.91 eV. Neglecting the free hole concentration of BST in comparison with the electrons concentration (oxygen vacancies) and assuming that $N_{tn} \approx 10^{18}$ cm^{-3}, the Fermi-quasi level for electrons is evaluated as 0.14 eV below the conduction band E_{c1} and thus the work function for BST becomes 4.04 eV ($n_{f1} \approx 10^{17} cm^{-3}$). As it is stated in [14-17], the mismatch of $SrTiO_3$ and $BaTiO_3$ with Si is ≈ 1.7% [17], therefore we had adopted low surface state concentration of about $6 \cdot 10^{10}$states/cm^2 eV. Taking into account the above mentioned data concerning BST/cp-Si, the band structure was constructed based on the Anderson model (Fig. 1). The conductance band offset is equal to

$$\Delta Ec = E_{c2} - E_{c1} - q\Phi_{B0} \text{or} \Delta Ec = [x_{BST} - x_{Si}] \approx \text{- 0.15 eV}$$

and the valence band offset is $\Delta Ev = [x_{BST} - x_{Si}] + [E_{gBST} - E_{gsi}] \approx$ 1.95 eV. As it follows from Fig.2 (based on the fact that the Fermi level must be constant throughout this system at thermal equilibrium), the built-in potential equals

$$q\Phi B_0 (= E_{g1}/2 \text{-} E_{g2} \text{-} \Delta Ec) \cong 0.61\ eV.$$

Beside inspection of the energy band diagram, the built-in potential $q\Phi_{B0}$ across interfacial layer can be obtained by application of the Gauss law to the surface charge on the BST and Si.

In this work, where we used the depletion approximation and for establishing the thermal equilibrium condition, the following mechanisms have been offered. As it has been assumed before, high oxygen vacancies in the BST interface and $x_{BST} < x_{Si}$, the free electron concentration in BST is larger than that of minority charge carriers (electrons) in p-Si ($n_{po} \approx 10^5$ cm^{-3}, $p_{po} \approx 2.10^{15}$ cm^{-3}). After formation of heterojunction, electrons will be diffused to the p-Si conduction band and recombined with holes. BST will be charged positively due to the increase of non-compensated oxygen vacancies associated with the donor-like charged trap levels and p - Si would be charged negatively. As ΔE_v is higher and as pc-Si holes act as potential barrier, holes cannot diffuse in the BST valence band. Holes from the BST valence band may pass heterojunction and drift to the pc-Si valence band. As BST is charged positively and p-Si-negatively, the barrier for electrons will be formed as well. We assume that the transition from the ordered pc-Si crystalline phase to the BST phase takes place on not more than several atomic distances [1, 8, 9], which is rapid enough to be considered as abrupt transition but not so sudden as to give a surface dipole.

Depletion layer. For calculation of the depletion layer widths, the distribution of built-in potentials, using the rule of continuality of electrostatic potential across the interface

$$\varepsilon_1 \frac{d\phi_1}{dx}\Big| x_B = \varepsilon_2 \frac{d\phi_2}{dx}\Big| x_s = 0 \tag{1}$$

as well as the expression of [10-12]

$$\varepsilon_1 = \frac{\varepsilon_0}{1+A\mathcal{F}^2} = \frac{\varepsilon_0 \varepsilon(0)}{1+A\mathcal{F}^2},$$

and assuming that the occupation function of the distribution of trapped electron can be approximated by step of 0 K Fermi function [18], for the depletion-layer charge density of the BST side, we obtain [12]

$$\rho_1(x) = \left\{N_{tn}[1-2f_t(\mathcal{F})] + p_{f1}(x) - n_{f1}(x) - N_{A1}^-\right\}, \tag{3}$$

where ε_1 and ε_2 are the BST and cp-Si sides depletion-layer dielectric permittivity, respectively, x_B and x_s correspond to the edges of depletion layers in both sides, $\Phi_1(x)$ and $\Phi_2(x)$ are the electrostatic potentials in BST and pc-Si depletion layers, respectively, $\boldsymbol{\mathcal{F}}$ (x) is the electric field in the BST depletion layer, $f_t(\varepsilon)$ is the field-dependent occupation function of trapped electrons, ε_0 is the vacuum dielectric constant ($8.85\cdot10^{-12}$ F/m), $\varepsilon(0)$ is the BST dielectric permittivity at zero electric field, x is the current coordinate.

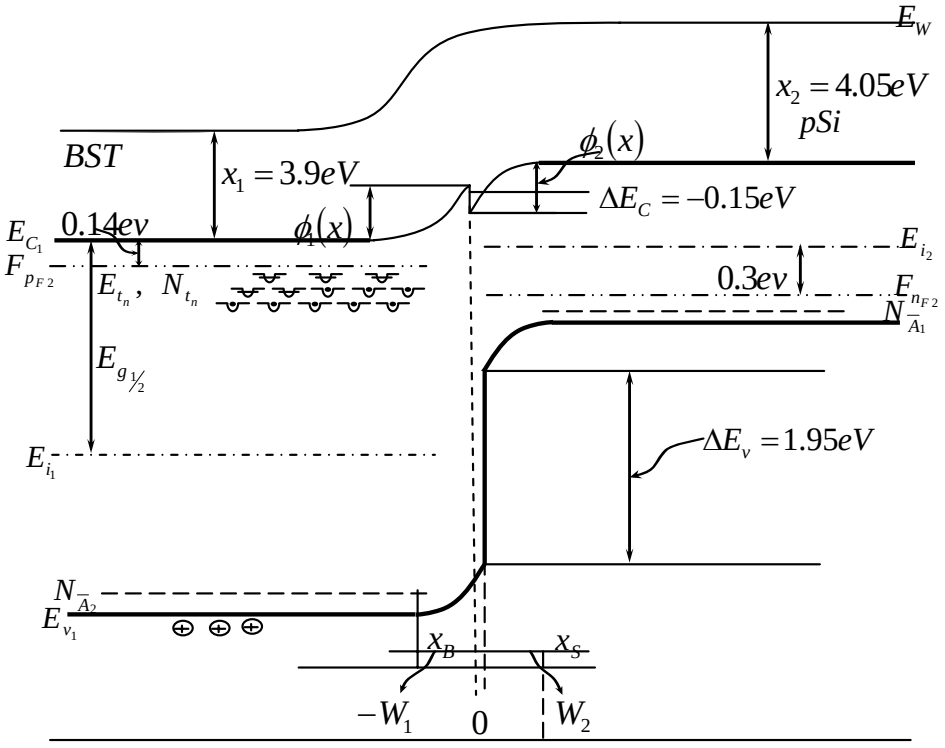

Fig. 2. Energy band diagram of the BST/cp-Si heterojunction.

The space charge density, $\rho_1(x)$, in the ferroelectric-depletion layer is determined by the density of non-compensated positively charged oxygen vacancy concentration, N^+_v, trapped electron

concentration, $n_{tn}(x)$, in the oxygen vacancies created trap levels, as well as by the density of acceptor like charges, N_{A1}, and free charge carriers $n_{f1}(x)$ and $p_{f1}(x)$ (see Fig. 2). For simplicity, let us assume that donor-like energy levels (conditioned by oxygen vacancies) can be approximated by the exponential term with the characteristic energy of E_{tn} and density of N_{tn} [19]:

$$N_{tn} = A_{tn} exp\left(-\frac{E_{tn}}{KT}\right), \tag{4}$$

where constant A_{tn} defines the shape of the distribution of traps in energy.

In the bulk of ferroelectric, far from the heterojunction surface, the charge neutrality must exist. Therefore $\rho_1(x) = 0$ and potential, $\Phi_{10}=0$, and we have

$$N_{A1}^{-} = N_{tn}[1 - 2f_t(0)] + n_{10} - p_{10} \ , \tag{5}$$

where $f_t(0)$, the occupation function before the heterojunction, is created and built-in potential (surface potential Φ_{10} and electric field Φ_1 appear), n_{10} and p_{10} are the bulk free concentration of electrons and holes in BST before the heterojunction is formed. For $f_t(0)$ we have [12]

$$f_t(0) = \frac{n_{10}S}{n_{10}S+\nu \exp(-\beta E_{tn})},$$

and under the built-in electric field (after creation of heterojunction) or under an applied external field , Φ, some electrons are released from the traps, and field-dependent distribution function $f_t(\Phi)$ becomes [12]

$$f_t(\mathcal{F}) = \frac{n_c S}{n_c S+\nu exp\left(-\frac{E_{tn}}{kT}+\beta_{PF}\sqrt{\mathcal{F}}\right)}. \tag{6}$$

Here $S = \sigma_s v_{tn}$, σ_s is the capture cross section, $v_{tn} = \left({}^{3KT}/_{m}\right)^{1/2}$ is the thermal velocity of the electrons, ν is the "attempt to escape" frequency which is connected to relaxation time with the relationship $\tau = \frac{1}{\nu}\exp(\beta E_{tn})$, and $\beta = q/KT$, q is the electron charge, k is the Boltzmann's constant and T is the absolute temperature, $\beta_{PF} = \frac{1}{KT}\sqrt{\frac{q^3}{\pi \varepsilon_0 \varepsilon_{0pt}}}$ is the Pool-Frenkel coefficient (barrier lowering factor), ε_{opt} is the optical limited permittivity of ferroelectric and characterizes only the charge de-trapping process, not the dielectric permittivity at low or microwave frequencies.

Taking into account (4) and (5) we obtain for the expression (3):

$$\rho_1(x) = q\{N_{tn}.2[f_t(0) - f_t(\mathcal{F})] + p_{f1}(x) - p_{10}(x) - n_{f1}(x) + n_{10}(x)\}. \tag{7}$$

The electron and hole concentrations as a function of surface potential of the BST side, Φ_{10}, is given by the following relations:

$$n_{1f}(x)=n_{10}\exp(\beta\Phi_1(x)),\ p_{1f}(x)=p_{10}\exp(-p\Phi_1(x)),$$

$$n_{10} = N_{c1} exp\left[\frac{F_{nF1}-E_{c1}}{kT}\right],\ P_{10} = N_{v1} exp\left[\frac{F_{v1}-E_{PF1}}{kT}\right],$$

where $\Phi_1(x)$ is the electrostatic potential in the BST side depletion layer, N_{c1} and N_{v1} are the effective densities of states in the conduction and valence band of BST, respectively, F_{nF1} and F_{PF1} are the Fermi quasi levels for the electrons and holes, respectively.

Thus, for $\rho_1(x)$ we obtain:

$$\rho_1(x) = q\{2N_{tn}[f_t(0) - f_t(\mathcal{F})] + p_{10}(e^{-\beta\Phi_1(x)} - 1) - n_{10}(e^{\beta\Phi_1(x)} - 1)\}. \quad (8)$$

Taking into account a non-linear dependence of the ferroelectric dielectric permittivity on the electric field, we have for the Poission equation

$$\frac{d[\varepsilon_1(\mathcal{F}_1, x)\mathcal{F}_1(x)]}{dx} = \rho_1(x),$$

where$\mathcal{F}_1(x)$ is the built–in-field in the BST depletion layer, $\varepsilon_1(\mathcal{F}_1, x)$ is the BST dielectric permittivity.

The solution of Eq. 9 with the boundary conditions x=0, $\Phi_1 = \Phi_{10}$ gives

$$W_1 \cong \left\{\frac{\eta_{r\Phi_{10}} S n_{10} \exp(\beta E_{tn})}{q N_{tn}(1+C_{PF})\nu}\right\}^{\frac{1}{2}}, \quad (10)$$

where $C_{PF} = \exp(\beta_{PF}\mathcal{F}_{10}^{1/2})$.

As follows from expression (10), with the increase in N_{tn} (i.e. concentration of oxygen vacancies), the depletion-layer width, w_1, will be decreased. As large E_{tn}, i.e. as the trap levels become deep, the concentration of free electrons will be decreased and, hence, w_1 increased.

In the p - Si side depletion layer for the space charge, $\rho_2(x)$, we have

$$\rho_2(x) = q\{-N_{A2}^- + P_{f2}(x) - n_{2f}(x)\},$$

where N_{A2}^- is the acceptor concentration, $P_{2f}(x)$ and $n_{2f}(x)$ are the free hole and electron concentrations, respectively, and

$$n_{f2}(x) = n_{po}exp(\beta\Phi_2(x)),\ n_{po} = N_{c2}exp\left(\frac{F_{nF2} - E_{c2}}{kT}\right),\ P_{f2}(x) = P_{Po}\exp(-\beta\Phi_2(x)),$$

$$P_{po} = N_{v2}exp\left(\frac{E_{v2} - F_{PF2}}{kT}\right).$$

Here N_{c2}, N_{v2} are the effective densities of states at the conduction and valence bands, F_{nF2} , F_{PF2} are the electron and hole quasi-Fermi levels and $\Phi_2(x)$ is the electrostatic potential on the pc-Si side, respectively.

Solving the Poission's equation for the pc-Si depletion layer with the boundary conditions:

$$x = W_2, \qquad \Phi_2(x) = 0, \qquad x = 0, \qquad \Phi_2(x) = /\Phi_{20}/,$$

we obtain

$$W_2 = (\frac{2\varepsilon_2}{q\beta P_{po}})^{1/2}[\ln/1 + \beta\Phi_{20}/]^{1/2} \cong (\frac{2\varepsilon_2\Phi_{20}}{qP_{po}})^{\frac{1}{2}} \quad . \tag{11}$$

If μ_1 is chemical potential on BST side and μ_2 the chemical potential on the p - Si before the contact of both materials, we have (Fig.1)

$$q\Phi_{B0} = \mu_2 - \mu_1 - \Delta E_c + E_{g1/2} - E_{g2},$$

where μ_1 refers to the energy in the middle of BST gap (that is $E_{c1} = E_{g1/2}$ and $E_{v1} = -E_{\boldsymbol{g1}}/2$**)** and μ_2 refers to the top of p - Si valence band, $E_{v2,}E_{g1,}E_{g2}$ are the BST and Si gaps, respectively, $\Delta E_c \cong x_1 - x_2$ and Φ_{B0} is the heterojunction built-in-potential in thermodynamic equilibrium. The chemical potential is determined from the charge neutrality condition in the bulk of the BST $(\rho_1(x) = 0)$, by an iterative procedure. The chemical potential μ_2 can be evaluated with the well known crystalline semiconductor equations. Under non-equilibrium condition $\Phi = \Phi_{B0} - V$, where V is the applied bias and $\mu_2 = F_{PF2}$, $\mu_1 = F_{nF1}$, $F_{pF1} = \mu_1 + qV$, $F_{nF2} = \mu_2 - qV$.

Using the condition for charge neutrality and equations (10) and (11) as well as

$$\Phi_{10} + \Phi_{20} = \Phi_{\beta 0}, \quad |W_1| + W_2 = W$$

for W we obtain

$$W = \sqrt{\frac{(\Phi_{\beta 0} - V)\varepsilon_r\varepsilon_2 d_1 d_2(\rho_1+\rho_2)^2}{\rho_2^2 d_2\varepsilon_2 + \rho_1^2 d_1\varepsilon_r}}, \tag{12}$$

where

$$d_1 = \frac{n_{10}Sexp(\beta E_{tn})}{qN_{tn}(1 + C_{PF})\nu} \quad , \qquad d_2 = \frac{2}{qp_{po}}$$

If we have homo abrupt p-n junction,

$$\varepsilon_r = \varepsilon_2 = \varepsilon_{s,} \qquad \rho_1 \cong qN_d, \qquad \rho_2 = qN_A\,, \qquad d_1 = \frac{2}{qN_d}, \quad d_2 = \frac{2}{qN_A},$$

from expression (12) one can obtain well-known formula [20]

$$W_{P-n} = \sqrt{\frac{2\eta_S\Phi_{B0}(N_d + N_A)}{qN_dN_A}}.$$

3. Discussion

As it follows from (12), the heterojunction depletion width depends on both BST and pc-Si sides dielectric permittivities, as well as oxygen vacancies concentration (through to $\rho_1(x)$, N_{tn}) and doping density of pc-Si. The dependence of W on the above mentioned parameters are shown in

Fig. 3 and Fig. 4. The calculations have been carried out for the following parameters listed in Table 1, and: E_{tn}= 0.026…0.26 eV, C_{pF}= 0.1; Φ_{B0}= 0.6 V; $\eta(0)$ = 100…300; P_{p0}= $2\cdot10^{15}$ cm^{-3}; N_{tn}= (10^{15}…..10^{19})cm^{-3}; σ_s = 10^{-14} cm^2; $v_{tn} = 10^7$ cm/s; V = (-0.6…+0.6) V. With increase in N_{tn} which is connected with increasing concentration of oxygen vacancies and hence the concentration of free electrons in BST side, the depletion width decreases (Fig. 3). The depletion layer decreases with the increase of energy depth of trap levels, E_{tn}, (Fig. 4).

Table 1. Material parameters

	E_{g1}, BST	E_{g2}, pc-Si	ΔE_c, eV	ΔE_v,eV
Band gap, eV	3.2	1.1	-0.15	1.95
dielect. permit.	200-300	11.8	-	-
electron affinity, x_{BST}, x_{Si},eV	3.9	4.05	-	-
work function, eV	4.04	4.91		
Fermi quasi-level $E_{c1}-E_{nF1}$, eV $E_{pF2}-E_{v2}$, eV	0.14	0.31		
Chemical potential $\mu_1(E_{g1}/2-F_{nF1})$, eV $\mu_2(E_{C2}-0.85)$, eV	1.46	1.2		

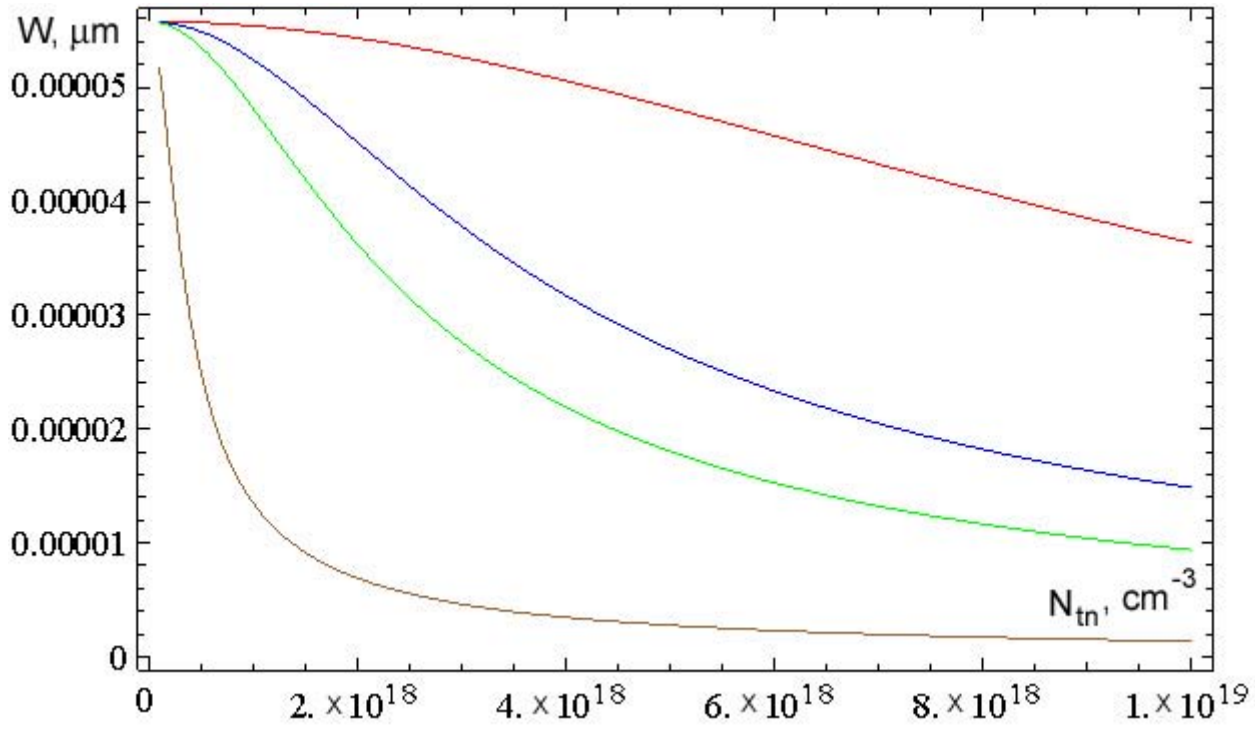

Fig.3. Dependence of the depletion layer width, W, on the oxygen vacancies concentration, N_{tn}, for different values of E_{tn} (the other parameters are: v=0 V, C_{pF}=0.1, Φ_{B0}=0.6 V, ε(0)=100, P_{P0}=$2\cdot10^{15}$ cm-3).

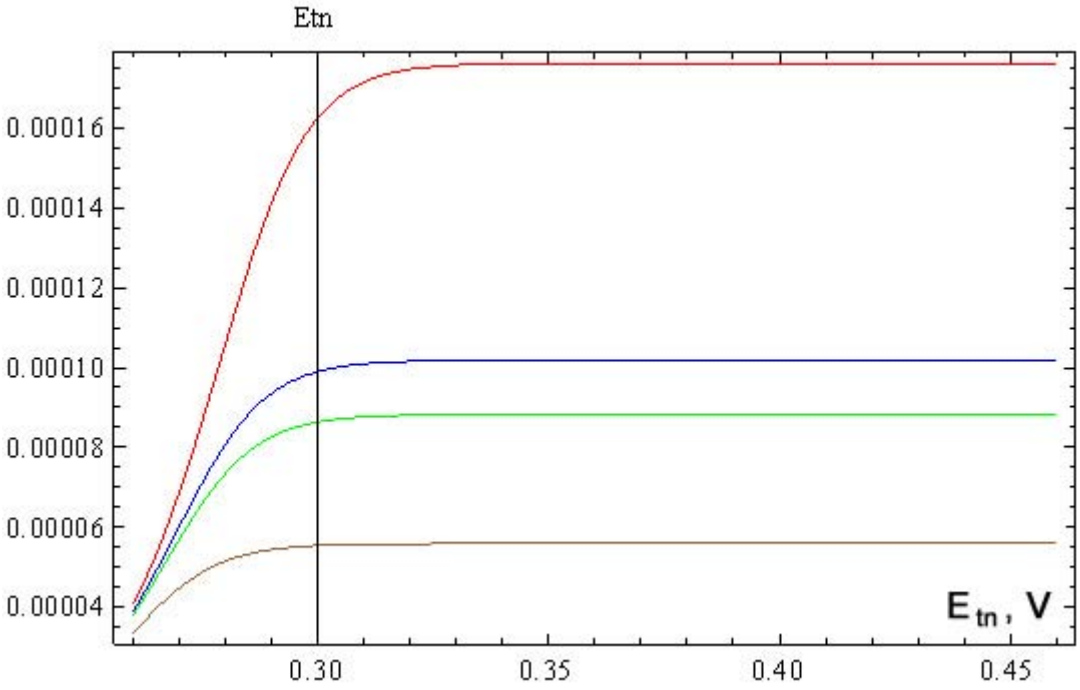

Fig. 4. Dependence of the depletion layer width, W (cm), on E_{tn} for different values of P_{p0} (cm^{-3}) (the other parameters are: v = 0 V, $N_{tn} = 10^{17} cm^{-3}$, and as in Fig. 3)

This work was supported by State Committee of Science MES RA, in the frame of the research project *№ SCS 13-2G032.*

R E F E R E N C E S

1. F. Amy, A.S. Wan, and A.Kahn, et al. Band offsets at heterojunctions between $SrTiO_3$ and $BaTiO_3$ and Si(100). J. Appl. Phys., 96, 1635 (2007).
2. Z. Luo, J.H. Hao, J. Gao. Rectifying characteristics and transport behavior of $SrTiO_{3-\delta}$ (110)/pSi (100) heterojunctions. Appl. Phys. Lett., v.91, pp.91.062105-1-3, 2007.
3. J. Huang, K. Zhao, H. Lu et al. Characteristics of heterojunctions of amorphous $LaAlO_{2.73}$ on Si. Physica B, 373, 313, (2006).
4. Ch.-l Hu, P. Han, K. Jin et al. Theoretical study of the transport property of p-Si/n $SrTiO_{3-\delta}$. J. App. Phys., v.103, p103, 053701, 2008.
5. Z. Ling, C. Leach, R. Fzeer. Heterojunction gas sensors for environmental NO_2 and CO_2 monitoring, J. of European Ceram.Society, v.21, pp.1977-1980, 2001.
6. C.H.Park, D.J. Chadi. Phys. Rev. B57, p.13961, 1998, Microscopic study of oxygen vacancy defect in ferroelectric perovskite; J. Appl. Phys.v.92, N11, pp.6778-6786, Modelling the role of oxygen vacancy on ferroelectric properties.
7. M. Dawber, J. F.Raba, J.F.Scott. Physics of thin film ferroelectric oxides. Rev. of Modern Phys., v.77, pp 1083-1130, 2005.
8. J.Robertson, Energy levels of point defects in $SrTiO_3$ and related oxides, J.Appl. Phys. v. 93, N2, pp.1054-1059, 2003.
9. J.Robertson. Interfaces and defects of high-K oxides on silicon. Solid State Electronics, v.49, pp.283-293, 2005.
10. M. Dawber, J.F. Raba, J.F.Scott. Physics of thin-film ferroelectric oxides. Rev. of Modern Phys., v.77, pp.1083-1130, 2005.
11. A.K.Tagantsev, V.O. Sherman, K.F. Astafiev et al. Ferroelectric materials for microwave tunable applications, J. Electroceramics., v.11, pp. 5-66, 2003.

12. V. V.Buniatyan, N. W. Martirosyan, A. K. Vorobiev et al. Dielectric model of point charge defects in insulating paraelectric perovskites. J. Appl. Phys., v.110, pp. 09410-1-11, 2010.
13. C. Jia, J. Chen, J. Guo et al. Valence band offset of InN/$BaTiO_3$ heterojunction measured by X-ray photoelectron spectroscopy. NanoscaleResarch Letters, v.6, pp.316-1-5, 2011.
14. S.A.Chambers and Y.Liang, Z.Yu et al. Band discontinuities at epitaxial SrTiO3/Si(001) heterojunctions. Appl. Phys., letters, 77,1662(2000)
15. K.F. Brennan, A. S. Brown, Theory of modern electronic semiconductor devices, Wiley Interscience, 2002.
16. C.J. Forst, C.R. Ashman, K. Schwarz et al. The interface between silicon and a high-k oxide. Nature, v.427, N1, pp.53-56, 2004.
17. P.W. Peacock and J. Robertson. Band offsets and Schottky barrier heights of high dielectric constant oxides. J. Appl. Phys., v.92, pp.4712-4721, 2002.
18. M.S.Shur, W.Gzubatyj and A.Madan. Schottky barrier profiles in a-Si based materials. J.Non-Crystal. Solids, v.35-36, part 2, pp.731-736, 1980.,
19. M. Lampert, P. Mark, Current injection in solids, Acad., Press, p.416 (1970).
20. S.M.Sze Physics of Semiconductor Devices, 3rdedn., Wiley Interscience, 898, (2006).